

ALMA: Aggregated Lipschitz Maximization Attack on Auto-encoders

Chethan Krishnamurthy Ramanaiik, Arjun Roy, Eirini Ntoutsis

University of the Bundeswehr Munich, Germany

{chethan.krishnamurthy, arjun.roy, eirini.ntoutsis}@unibw.de

Abstract

Despite the extensive use of deep autoencoders (AEs) in critical applications, their adversarial robustness remains relatively underexplored compared to classification models. AE robustness is characterized by the Lipschitz bounds of its components. Existing robustness evaluation frameworks based on white-box attacks do not fully exploit the vulnerabilities of intermediate ill-conditioned layers in AEs. In the context of optimizing imperceptible norm-bounded additive perturbations to maximize output damage, existing methods struggle to effectively propagate adversarial loss gradients throughout the network, often converging to less effective perturbations. To address this, we propose a novel layer-conditioning-based adversarial optimization objective that effectively guides the adversarial map toward regions of local Lipschitz bounds by enhancing loss gradient information propagation during attack optimization. We demonstrate through extensive experiments on state-of-the-art AEs that our adversarial objective results in stronger attacks, outperforming existing methods in both universal and sample-specific scenarios. As a defense method against this attack, we introduce an inference-time adversarially trained defense plugin that mitigates the effects of adversarial examples. Code repo: <https://github.com/ChethanKodase/alma>

1. Introduction

Autoencoders (AEs) [9, 18, 27, 34] are neural networks that learn unsupervised representations by encoding input data into a lower-dimensional latent space and reconstructing it. They form the backbone of modern scientific computing in tasks such as image compression, denoising, anomaly detection, and generative modeling [12, 33]. Given their increasing deployment in high-stakes domains, it is crucial to rigorously evaluate their adversarial robustness. However, unlike classification models—where adversarial vulnerabilities have been extensively explored [14, 31]—adversarial attack methodologies targeting AEs remain comparatively underdeveloped. One key challenge is that AEs do not pre-

dict discrete classes but instead optimize reconstruction objectives [32], making many classification-based adversarial strategies difficult to adapt directly.

Recent research indicates that adversarial perturbations for AEs can be more perceptible than those for classifiers [11, 20, 22, 36]. In part, this arises from vanishing gradients in the backpropagation chain due to ill-conditioned Jacobians, a phenomenon tied to the lack of dynamic isometry [26]. Specifically, layers with very low Jacobian singular values introduce near-singular Jacobians that yield negligible gradient updates, limiting the efficacy of many standard attack methods. A similar effect has been reported in quantized networks [16], where ill-conditioned Jacobians generate the illusion of adversarial robustness by impeding forward-backward signal propagation. Although [16] propose a method to mitigate this for classification models, it crucially depends on logits and class predictions, making it unsuitable for AEs. In parallel, studies on instabilities in deep inverse problems [3, 4] and the accuracy-stability trade-off [15] demonstrate that deep learning pipelines, including autoencoders, can exhibit severely ill-conditioned kernels. We thus hypothesize that the apparent robustness of AEs to naive gradient-based attacks is similarly attributable to vanishing gradients caused by ill-conditioned layers.

Prior works [1] suggest that the robustness of any neural network is closely related to Lipschitz continuity. Moreover, recent studies show that certifiable robustness of AEs depends on multiple factors, including the Lipschitz constants [17] of both the encoder and decoder [5]. This connection highlights the importance of understanding how adversarial perturbations interact with the Lipschitz properties of AEs, particularly in the presence of ill-conditioned layers. Consequently, in this work, we focus on gradient-based white-box untargated adversarial attacks on AEs that learn smooth latent representations, aiming to address these signal propagation challenges.

Our Contributions. Although ill-conditioned autoencoders (AEs) are likely to harbor potent adversarial examples, classical gradient-based attacks struggle to uncover them due to poor gradient signal propagation. Motivated

by this limitation, we propose a new attack framework that overcomes these challenges and reveals stronger adversarial vulnerabilities.

1. **Lipschitz Maximization Attack (LMA):** Addresses *decoder-side ill-conditioning* by introducing a latent-space mismatch term, overcoming vanishing gradients in the decoder.
2. **Aggregated Lipschitz Maximization Attack (ALMA):** Generalizes LMA by treating the autoencoder as multiple encoder–decoder splits, weighting each split *inversely* to its condition number. This mitigates vanishing gradients by down-weighting ill-conditioned AE layer interfaces and amplifying well-conditioned ones.
3. **Theoretical Analysis:** We prove that LMA mitigates vanishing gradients in ill-conditioned decoders, while ALMA extends this to cases where ill-conditioned layers occur anywhere in the model, ensuring efficient adversarial optimization.
4. **Empirical Validation:** ALMA outperforms existing attacks across multiple AEs, achieving faster convergence and greater reconstruction damage, offering a robust assessment of AE vulnerability.
5. **Defense via Adversarial Filter Plugins (AFP):** To counter ALMA, we introduce AFP—lightweight per-layer filters that operate at inference time without modifying AE parameters, effectively mitigating adversarial perturbations for cleaner reconstructions.

2. Related Work

Gradient-Based Adversarial Attacks on Autoencoders. White-box adversarial attacks optimize norm-bounded perturbations with full access to the target model, aiming to alter reconstruction or model decisions. Attacks can be *targeted*, steering reconstructions toward a specific target, or *untargeted*, maximizing reconstruction distortion without a predefined outcome.

Existing approaches primarily optimize perturbations to maximize the shift in latent representations using symmetric KL divergence [6, 21] or Wasserstein distance [8], which approximates to the norm of the Jacobian-perturbation product [21]. Additionally, some methods perturb the latent space directly for both targeted and untargeted attacks [25]. However, in this work, we focus exclusively on input-space perturbations. In adversarial attacks on Stable Diffusion models, cosine similarity is a commonly used metric for adversarial objectives [28, 37, 38]. Similarly, it is employed in adversarial optimizations targeting NSFW content generation in diffusion models [37, 38].

Summarizing gradient-based adversarial attacks on autoencoders, we find that these methods typically maximize the distance between latent representations or output reconstructions using L2 norm, Wasserstein distance, symmetric KL divergence, or cosine similarity.

Effects of Ill-Conditioning on Adversarial Optimization. Compared to classification models, adversarial perturbations on autoencoders are significantly more perceptible [11, 20, 22, 36]. This can be attributed to vanishing gradients caused by ill-conditioned Jacobians in the back-propagation chain [26]. Ill-conditioned layers hinder gradient flow, leading to ineffective perturbations, as observed in quantized networks [16]. While [16] propose techniques to mitigate this issue in classification models, their approach depends on class predictions, making it unsuitable for autoencoders. Autoencoders, like other deep learning models, are prone to instabilities in inverse problems [3, 4]. Theoretical work on accuracy-stability trade-offs [15] shows that deep learning models can develop ill-conditioned kernels, which may explain the apparent robustness of autoencoders against conventional gradient-based attacks.

To address this, we introduce a novel adversarial objective that tackles the gradient signal propagation problem while exploiting model instabilities caused by ill-conditioning, thereby crafting more effective adversarial attacks on autoencoders.

3. Preliminaries and Background

Among the numerous adversarial attacks explored in the literature [2], we focus on *untargeted white-box attacks*, where adversarial examples are generated by learning norm-bounded perturbations. These attacks require full access to the model’s parameters and gradients are computed across the model to optimize the adversarial perturbations.

To understand how these attacks impact learned representations, we focus on state-of-the-art `Auto-Encoders` (AEs), such as β -VAE [18], TC-VAE [9], hierarchical NVAE [34], and diffusion AE [27]. These models extend vanilla AEs in different ways: β -VAE enforces disentangled representations by introducing a regularization term, TC-VAE penalizes total correlation between latent variables to improve latent space disentanglement, hierarchical NVAE introduces structured latent variables for better expressivity, VQ-VAE replaces the continuous latent space with a discrete codebook, and diffusion AE integrates diffusion models for enhanced robustness and generation quality. However, we focus only on models that learn smooth representations, as our method is primarily designed to address gradient signal propagation issues caused by ill-conditioned Jacobians in the backpropagation chain while optimizing white-box maximum damage attacks on autoencoders.

Formal Setup. We assume an image dataset $\mathcal{I} = \{x\}$, $x \in \mathbf{R}^{h \times w}$ for h height and w width. Let \mathcal{Y} be a target deep visual autoencoder (AE) model, consisting of an encoder function $\phi(\cdot)$ and a decoder function $\psi(\cdot)$. The reconstruction process is defined as [13]: $\mathcal{Y}(x) = \psi(\phi(x))$

The AE \mathcal{Y} is trained to learn an optimal mapping $X \rightarrow X'$, ensuring that the reconstructed image $X' = \psi(\phi(X))$

closely resembles the original, i.e., $X' \approx X$.

Given a distance metric Δ , an AE \mathcal{Y} is robust if small perturbations $\delta(x, x_a)$ to input x to generate x_a (constrained within $\mathbf{B}_c^p(x)$ the L_p ball of x with radius c) do not significantly change its output:

$$\Delta(\mathcal{Y}(x_a), \mathcal{Y}(x)) \approx 0, \quad (1)$$

$$\text{where } x_a \in \mathbf{B}_c^p(x) = \{x' \in \mathbb{R}^{h \times w} \mid \|x - x'\|_p \leq c\}$$

Our goal is to find the optimal adversarial attack x_a^* that maximizes the reconstruction error:

$$x_a^* \leftarrow \operatorname{argmax}_{x_a \in \mathbf{B}_c^p(x)} \Delta(\mathcal{Y}(x_a), \mathcal{Y}(x)) \quad (2)$$

We refer to the objective in Eq. 2 as Output attack. To optimize the objective we use the gradient descent algorithm to update x_a at every training step as:

$$x_a \leftarrow x_a + \eta \nabla_{x_a} \Delta(\mathcal{Y}(x_a), \mathcal{Y}(x)), \quad (3)$$

where η is a learning rate, and ∇_{x_a} is the gradient of the objective w.r.t. x_a .

Role of Lipschitz Continuity. Robustness of any neural network is closely related to Lipschitz continuity. Assuming differentiability Lipschitz constant of AE [1] is: $\mathbf{L}_{\mathcal{Y}} = \sup_x \|\mathbf{J}_x^{\mathcal{Y}(x)}\|$ where $\mathbf{J}_x^{\mathcal{Y}(x)}$ is the Jacobian matrix capturing how the model output $\mathcal{Y}(x)$ changes with respect to input variations x .

Using the first-order approximation [21], the output difference can be expressed as $\Delta(\mathcal{Y}(x_a), \mathcal{Y}(x)) = \|\mathbf{J}_x^{\mathcal{Y}(x)} \delta(x_a, x)\|$ and the output attack objective in Eq. 2 as:

$$x_a^* \leftarrow \operatorname{argmax}_{x_a \in \mathbf{B}_c^p(x)} \|\mathbf{J}_x^{\mathcal{Y}(x)} \delta(x_a, x)\| \quad (4)$$

which means that the adversary exploits the directions where Local Lipschitz constant (i.e., the norm of the Jacobian) is high to cause maximum output change.

Impact of Ill-Conditioned Jacobians. Since $\mathcal{Y}(x)$ is a composition of functions, i.e., $\mathcal{Y}(x) = f_n \circ f_{n-1} \circ \dots \circ f_1(x)$, if in Eq. 3 $\Delta(\mathcal{Y}(x_a), \mathcal{Y}(x)) = \|\mathcal{Y}(x_a) - \mathcal{Y}(x)\|^2$ the gradient of the adversarial objective can be expressed as $\nabla_{x_a} \Delta(\mathcal{Y}(x_a), \mathcal{Y}(x)) = 2 \cdot (\mathcal{Y}(x_a) - \mathcal{Y}(x))^T \cdot \nabla_{x_a} \mathcal{Y}(x_a)$ where

$$\nabla_{x_a} \mathcal{Y}(x_a) = \mathbf{J}_{f_{n-1}}^{\mathcal{Y}} \cdot \mathbf{J}_{f_{n-2}}^{f_{n-1}} \dots \mathbf{J}_{x_a}^{f_1}. \quad (5)$$

An intermediate layer f_k is said to be *ill-conditioned* if its Jacobian has a large condition number: $\kappa(f_k) = \frac{\sigma_{\max}(\mathbf{J}_{f_{k-1}}^{f_k})}{\sigma_{\min}(\mathbf{J}_{f_{k-1}}^{f_k})} \gg 1$. Such layers can cause:

- **Susceptibility to adversarial examples:** σ_{\max} large \Rightarrow small input change yields large output change.
- **Vanishing gradients:** $\sigma_{\min} \approx 0 \Rightarrow$ ineffective gradient signal during optimization converging to less effective adversarial examples.

Any ill-conditioned f_k such that $\sigma_{\min}(\mathbf{J}_{f_{k-1}}^{f_k}) \approx 0$, could result in insignificant $\nabla_{x_a} \mathcal{Y}(x_a)$ due to Eq. 5, hindering adversarial optimization. Addressing this gradient degradation motivates our approach, which we present in the next sections.

4. Lipschitz Maximization Attack

The problem formulated in Eq. 4 exploits the robustness of target AE \mathcal{Y} as any given neural network (NN). However, in Sec. 3 we see that AEs are special type of NNs with a functional composition of encoder $\phi(\cdot)$, and decoder $\psi(\cdot)$, which can be viewed as separate NNs. Thus, in literature we see adversarial attacks optimizing for output [11] divergence (Eq. 4), as well only latent space [22] divergence i.e., concerning only the encoder, has been proposed.

Moreover, recent studies shows [5] that certifiable robustness of AEs depend on factors including:

- The Lipschitz constants [17] of the encoder and decoder.
- The norm of the encoder's deviation with respect to input perturbations.

Therefore, to completely exploit the robustness factors of \mathcal{Y} we need to maximize damage of the encoder $\phi(\cdot)$ by:

$$\operatorname{argmax}_{x_a \in \mathbf{B}_c^p(x)} \|\mathbf{J}_x^{\phi(x)} \delta(x_a, x)\| \quad (6)$$

and to maximize damage of the decoder $\psi(\cdot)$ by:

$$\operatorname{argmax}_{\phi(x_a) \mid x_a \in \mathbf{B}_c^p(x)} \|\mathbf{J}_{\phi(x)}^{\psi(\phi(x))} \delta(\phi(x_a), \phi(x))\| \quad (7)$$

Now, using Eq. 6, and 7, we modify the maximum damage attack criteria (c.f. Eq. 4), to define the Lipschitz Maximization Attack (LMA) on AEs as follow:

$$x_a^* \leftarrow \operatorname{argmax}_{x_a \in \mathbf{B}_c^p(x)} (\|\mathbf{J}_{\phi(x)}^{\psi(\phi(x))} \delta(\phi(x_a), \phi(x))\| \|\mathbf{J}_x^{\phi(x)} \delta(x_a, x)\|) \quad (8)$$

Following the discussion in Sec. 3, we can say that Eq. 8 is a first order approximation of:

$$x_a^* \leftarrow \operatorname{argmax}_{x_a \in \mathbf{B}_c^p(x)} \Delta(\mathcal{Y}(x_a), \mathcal{Y}(x)) * \Delta(\phi(x_a), \phi(x)) \quad (9)$$

The formulation in Eq. 9 in particular allows to design the adversary in such a way that vulnerability of the encoder and decoder both gets individually exploited. Vulnerability of a network during forward propagation can be identified using condition number [30] of the network. Specifically, the condition number $\kappa(\cdot)$ of the encoder, and the decoder can be estimated [10] by:

$$\kappa(\phi) = \frac{\sigma_{\max}(\mathbf{J}_x^{\phi(x)})}{\sigma_{\min}(\mathbf{J}_x^{\phi(x)})}, \quad \kappa(\psi) = \frac{\sigma_{\max}(\mathbf{J}_{\phi(x)}^{\psi(\phi(x))})}{\sigma_{\min}(\mathbf{J}_{\phi(x)}^{\psi(\phi(x))})} \quad (10)$$

where σ_{\min} and σ_{\max} are respectively the minimum and maximum singular values of the concerned Jacobian. Ideally, network with $\kappa(\cdot)$ close to 1 is considered as well-conditioned layer. A high value of $\kappa(\cdot)$ indicates an ill-conditioned (more vulnerable or less robust) network, and henceforth, expected to produce larger adversarial deviation for smaller input perturbation. While, a adversary ideally would like to exploit such ill-conditions, however, during optimization for the ideal perturbed image x_a^* within the constrained ball \mathbf{B}_c^p , such ill-conditioning makes the convergence problematic [23, 29]. Specifically, under ill-condition, the optimization of x_a^* will be hindered by vanishing [35] (when $\sigma_{\min} \rightarrow 0$), and exploding [19] (when $\sigma_{\max} \rightarrow \infty$) gradients.

Lemma 4.1. *Let $\phi(\cdot)$ be the encoder and $\psi(\cdot)$ be the decoder. Then Jacobian $\mathbf{J}_{\phi(x)}^\psi$ at $\phi(x)$ is such that $\sigma_{\min}(\mathbf{J}_{\phi(x)}^\psi) \rightarrow 0$, so that the decoder is ill-conditioned around $\phi(x)$. Let*

$$\begin{aligned} x_a^{OA} &\leftarrow \operatorname{argmax}_{x_a} \Delta(\mathcal{Y}(x_a), \mathcal{Y}(x)) \quad \text{and} \\ x_a^{LMA} &\leftarrow \operatorname{argmax}_{x_a} \Delta(\mathcal{Y}(x_a), \mathcal{Y}(x)) \Delta(\phi(x_a), \phi(x)), \end{aligned}$$

where Δ is a suitable distance (e.g. squared ℓ_1 - or ℓ_2 -distance). Then under the ill-conditioning assumption $\sigma_{\min}(\mathbf{J}_{\phi(x)}^\psi) \rightarrow 0$, the LMA (Lipschitz Maximization Attack) solution x_a^{LMA} typically attains a strictly larger output deviation. Formally,

$$\begin{aligned} \Delta(\mathcal{Y}(x_a^{LMA}), \mathcal{Y}(x)) &\geq \Delta(\mathcal{Y}(x_a^{OA}), \mathcal{Y}(x)), \\ \text{as } \sigma_{\min}(\mathbf{J}_{\phi(x)}^\psi) &\rightarrow 0. \end{aligned}$$

Proof. The proof is given in Appendix A. \square

From Lemma 4.1 we know that LMA is better way to learn adversaries than Output attacks when the later part of the model is ill-conditioned with low singular values of the decoder Jacobian, and this is also later empirically shown in Sec. 6.2.

5. Aggregated Lipschitz Maximization Attack

While LMA (Sec. 4) effectively addresses ill-conditioned decoders, it may still face difficulties if the encoders are themselves ill-conditioned (i.e., $\sigma_{\min}(\mathbf{J}_x^{\phi(x)}) \rightarrow 0$). In other words, if the gradient vanishes within the encoder, simply multiplying by the decoder Jacobian cannot recover a strong signal. Moreover, it can be the case that only a part of the decoder suffers from vanishing gradient, thus there is a possibility to still extract non-trivial useful adversarial update direction from the part in decoder beneath the ill-conditioned one.

To address the issue, we introduce **ALMA** (Aggregated Lipschitz Maximization Attack), which views the entire autoencoder \mathcal{Y} as an aggregation of multiple *encoder-decoder* pairs. Specifically, each “split” in the network is taken as:

- $\phi_k = f_k \circ f_{k-1} \circ \dots \circ f_1$, serving as an encoder up to layer k ,
- $\psi_k = f_n \circ f_{n-1} \circ \dots \circ f_{k+1} \circ \phi_k$, serving as a decoder from layer $k+1$ to n .

Hence, the original autoencoder $\mathcal{Y} = f_n \circ \dots \circ f_1$ can be interpreted as $n-1$ *encoder-decoder* configurations indexed by $k \in \{1, \dots, n-1\}$. Figure 1a illustrates this decomposition. Building on the layer-wise view, we quantify the adversarial deviation at layer f_k as:

$$\Delta(\phi_k(x_a), \phi_k(x)) \quad (11)$$

Inspired by LMA, our goal is to *jointly* maximize the deviation in the output space (i.e., $\Delta(\mathcal{Y}(x), \mathcal{Y}(x_a))$) and the intermediate-layer deviations $\Delta(\phi_k(x_a), \phi_k(x))$. However, to mitigate the problems of vanishing gradient in ill-conditioned encoders, we *weight* each layer’s contribution by a *linearly scaled inverse condition weighting* mechanism. Intuitively, layers that are well-conditioned (having a high minimum singular value but not exploding norms) will receive a higher weight, thus promoting stable gradient flow; whereas layers prone to vanishing or exploding signals are assigned lower weights, preventing them from dominating or nullifying the attack objective.

To formalize the weighting scheme, we define:

$$w_k = \frac{\sum_{j=1}^n \kappa(f_j) - \kappa(f_k)}{\sum_{j=1}^n \left(\sum_{i=1}^n \kappa(f_i) - \kappa(f_j) \right)}, \quad \text{for } k = 1, \dots, n-1 \quad (12)$$

where $\kappa(f_k)$ denotes the condition number of interface layer f_k . This formulation assigns lower weights to ill-conditioned (either vanishing or exploding) layers $\kappa(f_k)$, while boosting layers that have more reliable gradient propagation.

Aggregated adversarial objective. With the above weighting scheme, we extend LMA to an **aggregated** objective over all encoder-decoder pairs. Concretely, let $\phi_k(\cdot)$ and $\psi_k(\cdot)$ denote the respective splits for $k = 1, \dots, n-1$. Then we define:

$$\begin{aligned} x_a^* &\leftarrow \operatorname{argmax}_{x_a \in \mathbf{B}_c^p} \sum_{k=1}^{n-1} w_k \left\| \mathbf{J}_{x_a}^{\phi_k(x_a)} \Delta(x_a, x) \right\| \\ &\quad * \left\| \mathbf{J}_{\phi_k(x_a)}^{\psi_k(\phi_k(x_a))} \Delta(\phi_k(x_a), \phi_k(x)) \right\| \end{aligned} \quad (13)$$

In essence, we combine the *layer-wise* LMA objectives into a single aggregated loss. Our condition-number based weights w_k (c.f Eq. 12) *down-weight* those parts of the network that are ill-conditioned, focusing the adversarial perturbation where it can be reliably amplified without being

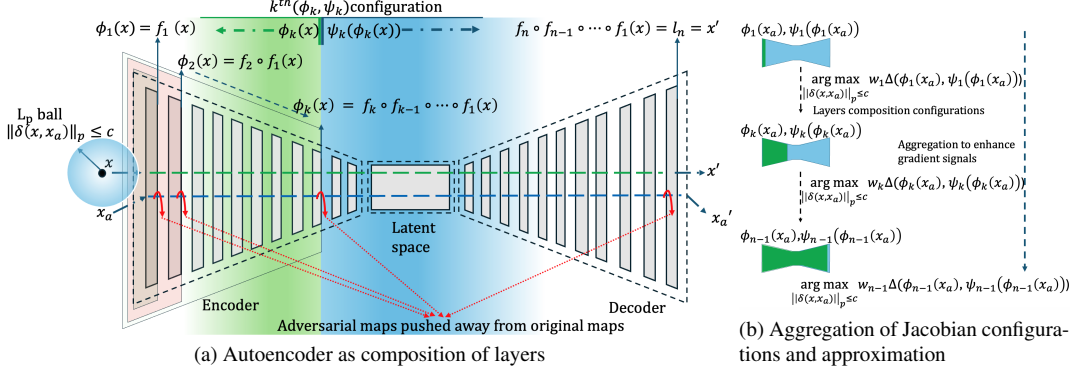


Figure 1. An overview of the ALMA attack pipeline

nullified or blowing up. Following Eq. 8 and Eq. 9 we can trivially arrive that the definition in Eq. 13 is a first order approximation of:

$$x_a^* \leftarrow \underset{x_a \in \mathcal{B}_c^p}{\operatorname{argmax}} \Delta(\mathcal{Y}(x_a), \mathcal{Y}(x)) \quad (14)$$

$$* \sum_{k=1}^{n-1} w_k \Delta(\phi_k(x_a), \phi_k(x))$$

Theorem 5.1. *Let the given the ALMA objective as in Eq. 14 is denoted by $\mathcal{F}(x_a)$, Output attack objective $\mathcal{G}(x_a)$, Latent attack objective $\mathcal{H}(x_a)$, an adversary x_a of an image x with x_a^* being the optimal adversary, and suppose there is an index $\ell \in \{1, \dots, n-1\}$ such that:*

1. $\sigma_{\min}(\mathbf{J}_x^{\phi_\ell(x)}) \geq \alpha_0$ for some constant $\alpha_0 > 0$.
2. For each $k < \ell$ at a given optimization step t ,
 $\|\phi_\ell(x_a)^{t-1} - \phi_\ell(x)\| \leq \|\phi_\ell(x_a)^t - \phi_\ell(x)\| \implies$
 $\|\phi_k(x_a)^{t-1} - \phi_k(x)\| \leq \|\phi_k(x_a)^t - \phi_k(x)\|$
3. $\sigma_{\min}(\mathbf{J}_x^{\phi_{\ell+1}(x)}) \rightarrow 0$.

Then, invoking Lemma 4.1 to address ill-conditioned decoders, we get:

1. $\|x_a^* - (x_a + \eta \nabla_{x_a} \mathcal{F}(x_a))\| \leq \|x_a^* - (x_a + \eta \nabla_{x_a} \mathcal{G}(x_a))\|$
2. $\|x_a^* - (x_a + \eta \nabla_{x_a} \mathcal{F}(x_a))\| \leq \|x_a^* - (x_a + \eta \nabla_{x_a} \mathcal{H}(x_a))\|$

Proof. The proof is given in Appendix B. \square

Theorem 5.1 mainly shows that if there exists at least one encoder layer ℓ with a non-vanishing Jacobian for $\Delta(\phi_\ell(x_a), \phi_\ell(x))$ and there is no perfect destructive interference from other layers, then even if other layers suffer vanishing gradients, ALMA maintains a nontrivial adversarial update direction.

6. Experiments

6.1. Experimental Setup

We conduct experiments on four state-of-the-art autoencoder models: β -VAE, TC-VAE, NVAE, and DiffusionAE,

to compare our proposed method, ALMA, with existing latent-space and output-space gradient-based attacks.

As mentioned in Section 2, we consider all relevant metrics found in the literature, including L2 distance, Wasserstein distance, symmetric KL divergence, and cosine distance. These metrics are used to compute the differences between the reference and original images in the latent space, output space, and intermediate layers during attack optimization, allowing a comprehensive evaluation of existing methods against our proposed ALMA method.

Following the standard in literature, we consider both universal and sample-specific adversarial attack scenarios across a range of perturbation magnitudes to analyze and compare the effectiveness of adversarial attacks.

We train the β -VAE and TC-VAE models on the CelebA dataset [24]. Additionally, we use official pretrained weights for NVAE (trained on CelebA) and DiffAE (trained on FFHQ256). However, due to the large size of NVAE and DiffAE and the high computational cost of full-scale attacks, we limit our focus to encoder-only attacks for these models, achieving efficient yet effective results. Consequently, output-space attacks (OA) and LMA are not applicable to NVAE and DiffAE. In our experimental setup, perturbations are optimized to solve the following adversarial attack objectives:

- **Latent Space Attacks (LA):** Maximizes the distance between the reference and adversarial latent representations. For NVAE, all hierarchical latent layers are attacked simultaneously, following [36].
- **Output Space Attack (OA):** Maximizes the MSE loss between the reference and adversarial outputs, as formulated in Eq. 2.
- **Lipschitz Maximization Attack (LMA):** Maximizes the product of MSE losses in latent and output spaces, enhancing adversarial effectiveness (Eq. 9).
- **Aggregated Lipschitz Maximization Attack (ALMA):** Our proposed layerwise adversarial objective, which optimizes perturbations across encoder-decoder splits

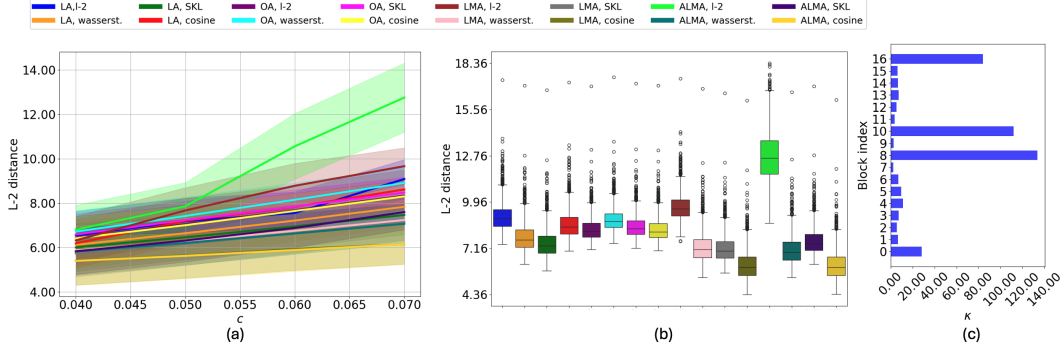


Figure 2. Comparison of universal adversarial attacks on β -VAE under $0.04 \leq c \leq 0.07$

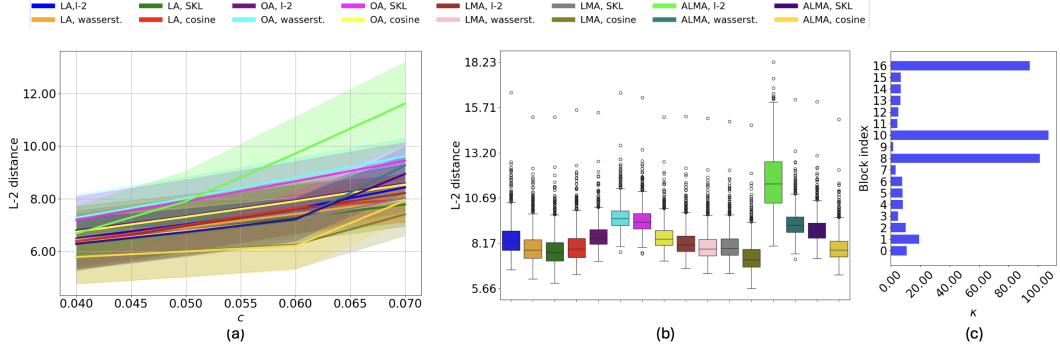


Figure 3. Comparison of universal adversarial attacks on TC-VAE under $0.04 \leq c \leq 0.07$

(Eq. 14).

Thus, our four adversarial objectives—**LA**, **OA**, **LMA**, and **ALMA**—combined with the four distance metrics—**L2**, **Wasserstein**, **Symmetric KL Divergence**, and **Cosine Distance**—result in 16 adversarial attack configurations. for the β -VAE and TC-VAE models, 8 adversarial configurations for NVAE and DiffAE. We also demonstrate adversarially trained inference time attack filter plugins to mitigate the effects of adversarial attacks.

6.2. Universal Attacks: A Comparison of Attack Methods Under a Fixed L_∞ Norm

We generate universal attacks by solving Eq. 14 for a single perturbation that applies to the entire dataset. This enables a fair, statistically significant comparison of each method’s effectiveness under fixed B_c^∞ norm constraints. We compare universal attacks using a set of 2000 samples per model.

6.2.1. Universal attacks on β -VAE and TC-VAE

For β -VAE and TC-VAE, Figures 2(a) and 3(a) show the distributions of output damages caused by all attack configurations across the range $0.04 \leq c \leq 0.07$. A common observation across both models is that ALMA (L-2) attacks outperform all other methods over a wide range of

B_c^∞ . However, at $c \leq 0.05$, the differences in attack performance are minimal, as the output damages in this range are insignificant and not comparable. Figures 2(b) and 3(b) reinforce this observation by providing a comparative analysis of output damage distributions for all attack configurations at $c = 0.07$.

For both β -VAE and TC-VAE, we conducted attacks using all four distance metrics for each method, and the tables report only the method-metric combinations that resulted in the highest output damage. Table 1 summarizes the mean and standard deviation of the highest-performing attack for each method. Across both models, the L-2 metric consistently outperformed SKL, Wasserstein, and cosine for latent attacks (LA). The wasserstein metric caused the highest output damage for output attacks, while the L-2 metric performed best for LMA and ALMA. Notably, ALMA with the L-2 metric achieved the highest output damage for both models, leading to a 40.41% increase over the best existing attacks for β -VAE. Although TC-VAE exhibits significant output damage under our ALMA (L-2) attack, its output damage increase is relatively lower at 22.98%, indicating greater robustness compared to β -VAE. This aligns with the findings of [36] and our observations of the condition numbers. Figures 2(c) and 3(c) illustrate the distribution of condition numbers across the layers of the trained β -VAE and

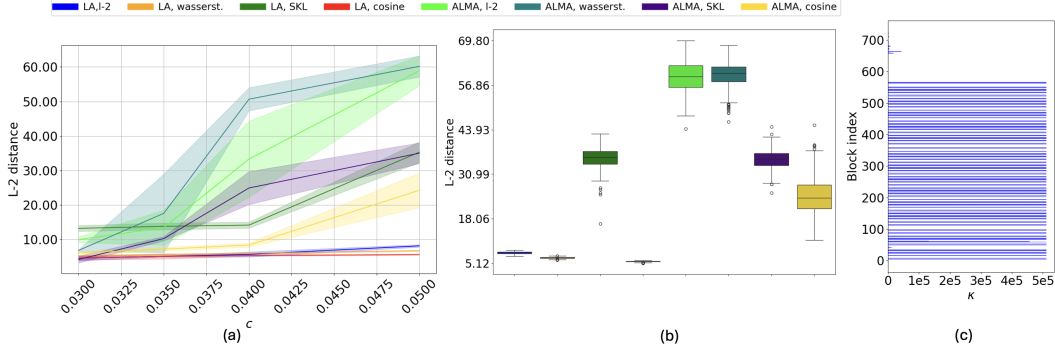


Figure 4. Comparison of universal adversarial attacks on NVAE under $0.03 \leq c \leq 0.05$

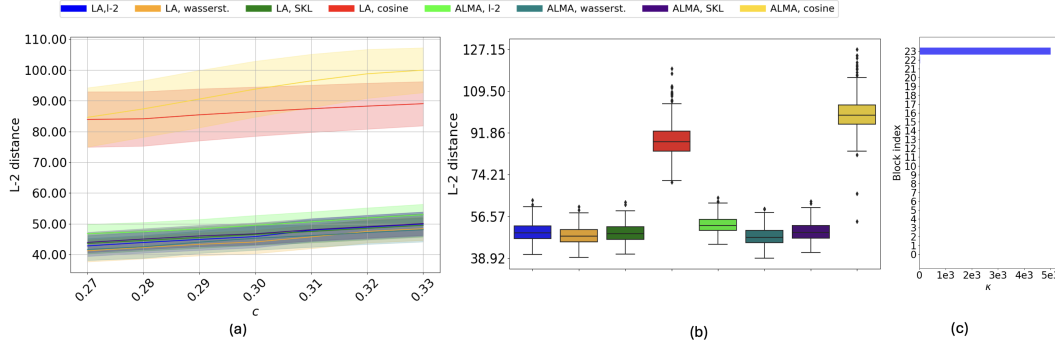


Figure 5. Comparison of universal adversarial attacks on DiffAE under $0.27 \leq c \leq 0.33$

TC-VAE, respectively. The range of condition numbers for β -VAE is relatively higher than that of TC-VAE, supporting our observation that TC-VAE demonstrates slightly greater resistance to ALMA attacks.

c	LA	OA	LMA	ALMA	Increase
≤ 0.07	L-2	Wass.	L-2	L-2	(%)
β -VAE	9.08 ± 0.87	8.91 ± 0.69	9.66 ± 0.82	12.75 ± 1.56	40.41
TC-VAE	8.42 ± 0.88	9.61 ± 0.68	8.21 ± 0.71	11.61 ± 1.57	22.98

Table 1. Mean and standard deviations output damage for β -VAE and TC-VAE

6.2.2. Universal attacks on NVAE

Figure 4(a) illustrates the output damage distribution across attack configurations for $0.03 \leq c \leq 0.05$. ALMA (Wasserstein) and ALMA (L-2) outperform all baselines for $c \geq 0.035$, with ALMA (SKL) also slightly surpassing existing methods. However, for $c \leq 0.035$, output damage differences remain negligible and not meaningful for comparison.

Table 2 reports the top-performing method-metric combinations. ALMA (Wasserstein) achieves a 68.63% increase in output damage over the strongest baseline. Figure 4(c) shows NVAE’s extensive ill-conditioned layers,

with some condition values capped at 5×10^5 for visualization.

This analysis highlights two key insights. First, severe ill-conditioning increases susceptibility to ALMA, as evidenced by the 68.63% rise in output damage at $c = 0.05$. Second, while ill-conditioned layers obstruct gradient propagation in conventional methods, weakening their attacks, ALMA circumvents this limitation, producing smaller yet highly effective universal perturbations that degrade reconstructions across a large number of samples.

c	LA	LA	ALMA	ALMA	Increase
≤ 0.05	L-2	SKL	L-2	wass.	(%)
NVAE	8.17 ± 0.38	35.64 ± 2.82	58.76 ± 4.56	60.10 ± 3.24	68.63

Table 2. Mean and standard deviations of output damage NVAE

6.2.3. Universal attacks on DiffAE

We focus on attacking only the encoder of the DiffAE model and compute layer-wise condition numbers, as shown in Figure 2(c). The results reveal that while most encoder layers are well-conditioned, ensuring efficient gradient propagation, the last layer is highly ill-conditioned.

c	LA	LA	ALMA	ALMA	Increase
≤ 0.33	L-2	cosine	L-2	cosine	(%)
DiffAE	49.94 ± 3.93	89.04 ± 7.17	52.96 ± 3.41	99.94 ± 7.29	12.24

Table 3. Mean and standard deviations of output damage DiffAE

Figure 5(a) shows that only LA (cosine) and ALMA (cosine) produce significant output damage, consistent with the frequent use of cosine similarity in adversarial attacks on diffusion-based models. Across the perturbation range $0.27 \leq c \leq 0.33$, ALMA (cosine) performs slightly better than LA (cosine), though both methods exhibit nearly identical performance at $c = 0.27$.

DiffAE demonstrates strong resistance to universal attacks, requiring higher perturbation levels compared to other models. This resilience is due to its well-conditioned layers, apart from the final ill-conditioned layer, which allows ALMA (cosine) to remain competitive with LA (cosine). The model’s higher image resolution (256×256 vs. 64×64) further increases the perturbation required for noticeable damage. However, as discussed in the next section, DiffAE remains highly vulnerable to untargeted attacks, even under imperceptible perturbations.

Figure 5(b) compares attack performance at $c = 0.33$, showing ALMA (cosine) achieving 12.24% higher output damage than LA (cosine), as quantified in Table 3.

Following [7], we evaluated Adam, gradient descent with momentum, and LBFGS for adversarial optimization. Adam provided faster convergence with nearly identical results to LBFGS, making it the preferred choice.

6.3. Sample-specific attacks: qualitative analysis

In this section, we analyze the qualitative effectiveness of adversarial attacks by evaluating sample-specific perturbations on autoencoders (AEs). Unlike universal attacks, which optimize a single perturbation for multiple inputs, sample-specific attacks tailor the perturbation individually for each input, providing a more precise measure of how effectively an attack exploits model vulnerabilities.

Figure 6 illustrates the impact of adversarial perturbations across all tested AEs. A striking observation is that ALMA consistently learns highly stealthy perturbations that remain visually imperceptible while causing significant distortions in reconstruction. This trend holds across all autoencoder models, including β -VAE, TC-VAE, NVAE, and DiffAE, demonstrating the effectiveness of ALMA in minimally perturbing the input while maximizing reconstruction damage. The difference in adversarial effectiveness becomes even more pronounced in larger-scale models such as NVAE and DiffAE. In these cases, ALMA yields the most damaging perturbations, leading to substantial output distortions, far exceeding those of baseline methods.

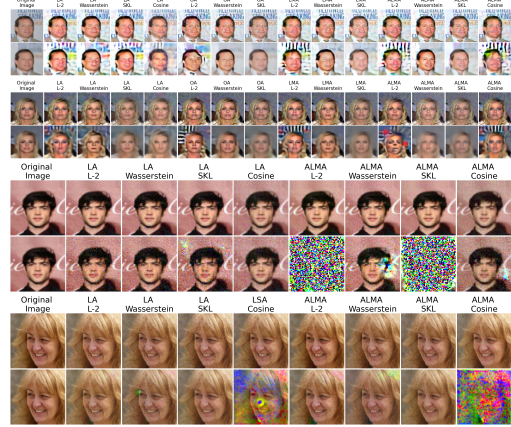


Figure 6. Sample-specific attacks (LMA, ALMA) vs. baselines on four AEs (top to bottom: β -VAE, TC-VAE, NVAE, DiffAE). Attack constraints: $c=0.07$ (β -VAE, TC-VAE), $c=0.04$ (NVAE), $c=0.08$ (DiffAE). In each model row, the top row shows perturbed inputs and the bottom row shows adversarial outputs.

This further highlights ALMA’s ability to overcome gradient vanishing issues coming from deeper layers and exploit ill-conditioned layers more effectively than other attacks.

6.4. Adversarial Filter Plug-in(AFP)

Tables 4 (NVAE) and 5 (DiffAE) highlight the effectiveness of our adversarial filter plug-in for mitigating adversarial output damage in NVAE and DiffAE. By inserting these filters before selected ill-conditioned layers and training them to suppress perturbations prior to final reconstruction, we disrupt the adversarial noise patterns crafted by the attacker. Consequently, the path of maximum damage is blocked, and as illustrated in Figures 7 and 8, our AFP largely nullifies the impact of these attacks.

LA, SKL damage($c=0.05$)		ALMA, wass. damage($c=0.05$)	
without filter	with filter	without filter	with filter
37.43	2.37	63.52	3.60

Table 4. Average output damage reduction of AFP for NVAE

LA, SKL($c=0.33$)		ALMA, wasserstein($c=0.33$)	
without filter	with filter	without filter	with filter
88.39	42.93	91.69	44.65

Table 5. Average output damage reduction of AFP for DiffAE

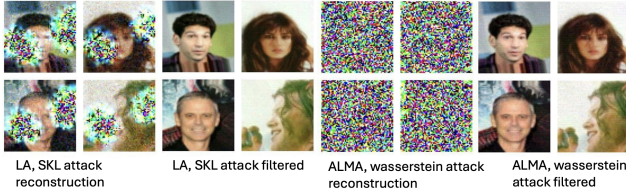


Figure 7. Inference time defense through AFP for attacks on NVAEs $c = 0.05$

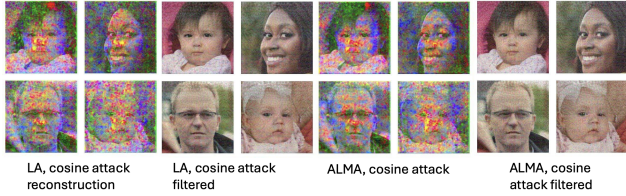


Figure 8. Inference time defense through AFP for attacks on Dif-fAEs $c = 0.33$

7. Conclusion

In conclusion, we clearly demonstrate that ALMA outperforms existing adversarial objectives for autoencoders. By comparing our method with established approaches across multiple model–metric combinations, we have shown that it consistently achieves superior adversarial impact. Furthermore, we prove both theoretically and empirically that ALMA ensures enhanced signal propagation and mitigates the problem of vanishing gradients caused by ill-conditioned Jacobians in the backpropagation chain. As our methodology is flexible enough to be adopted for any neural network architecture, it opens several promising directions for future work, including exploring additional emerging domains.

References

- [1] Abulikemu Abuduweili and Changliu Liu. Estimating neural network robustness via lipschitz constant and architecture sensitivity. *arXiv preprint arXiv:2410.23382*, 2024. 1, 3
- [2] Naveed Akhtar, Ajmal Mian, Navid Kardan, and Mubarak Shah. Advances in adversarial attacks and defenses in computer vision: A survey. *IEEE Access*, 9:155161–155196, 2021. 2
- [3] Vegard Antun, Francesco Renna, Clarice Poon, Ben Adcock, and Anders C Hansen. On instabilities of deep learning in image reconstruction and the potential costs of ai. *Proceedings of the National Academy of Sciences*, 117(48):30088–30095, 2020. 1, 2
- [4] Vegard Antun, Nina M Gottschling, Anders C Hansen, and Ben Adcock. Deep learning in scientific computing: Understanding the instability mystery. *SIAM NEWS MARCH*, 2021, 2021. 1, 2
- [5] Ben Barrett, Alexander Camuto, Matthew Willetts, and Tom Rainforth. Certifiably robust variational autoencoders. In *International Conference on Artificial Intelligence and Statistics*, pages 3663–3683. PMLR, 2022. 1, 3
- [6] Alexander Camuto, Matthew Willetts, Stephen Roberts, Chris Holmes, and Tom Rainforth. Towards a theoretical understanding of the robustness of variational autoencoders. In *International Conference on Artificial Intelligence and Statistics*, pages 3565–3573. PMLR, 2021. 2
- [7] Nicholas Carlini and David Wagner. Towards evaluating the robustness of neural networks. In *2017 IEEE Symposium on Security and Privacy (SP)*, pages 39–57. Ieee, 2017. 8
- [8] Taylan Cemgil, Sumedh Ghaisas, Krishnamurthy Dj Dvijotham, and Pushmeet Kohli. Adversarially robust representations with smooth encoders. In *International Conference on Learning Representations*, 2020. 2
- [9] Ricky TQ Chen, Xuechen Li, Roger B Grosse, and David K Duvenaud. Isolating sources of disentanglement in variational autoencoders. *Advances in neural information processing systems*, 31, 2018. 1, 2
- [10] Alan K Cline, Cleve B Moler, George W Stewart, and James H Wilkinson. An estimate for the condition number of a matrix. *SIAM Journal on Numerical Analysis*, 16(2): 368–375, 1979. 3
- [11] George Gondim-Ribeiro, Pedro Tabacof, and Eduardo Valle. Adversarial attacks on variational autoencoders. *arXiv preprint arXiv:1806.04646*, 2018. 1, 2, 3
- [12] Ian Goodfellow. *Deep learning*. MIT press, 2016. 1
- [13] Ian Goodfellow, Yoshua Bengio, and Aaron Courville. *Deep Learning*. MIT Press, 2016. <http://www.deeplearningbook.org>. 2
- [14] Ian J Goodfellow, Jonathon Shlens, and Christian Szegedy. Explaining and harnessing adversarial examples. *arXiv preprint arXiv:1412.6572*, 2014. 1
- [15] Nina M Gottschling, Vegard Antun, Anders C Hansen, and Ben Adcock. The troublesome kernel: On hallucinations, no free lunches, and the accuracy-stability tradeoff in inverse problems. *SIAM Review*, 67(1):73–104, 2025. 1, 2
- [16] Kartik Gupta and Thalaiyasingam Ajanthan. Improved gradient-based adversarial attacks for quantized networks. In *Proceedings of the AAAI Conference on Artificial Intelligence*, pages 6810–6818, 2022. 1, 2
- [17] William W Hager. Lipschitz continuity for constrained processes. *SIAM Journal on Control and Optimization*, 17(3): 321–338, 1979. 1, 3
- [18] Irina Higgins, Loic Matthey, Arka Pal, Christopher P Burgess, Xavier Glorot, Matthew M Botvinick, Shakir Mohamed, and Alexander Lerchner. beta-vae: Learning basic visual concepts with a constrained variational framework. *ICLR (Poster)*, 3, 2017. 1, 2
- [19] Sekitoshi Kanai, Yasuhiro Fujiwara, and Sotetsu Iwamura. Preventing gradient explosions in gated recurrent units. *Advances in neural information processing systems*, 30, 2017. 4
- [20] Asif Khan and Amos Storkey. Adversarial robustness of vaes through the lens of local geometry. In *International Conference on Artificial Intelligence and Statistics*, pages 8954–8967. PMLR, 2023. 1, 2

- [21] Anna Kuzina, Max Welling, and Jakub M Tomczak. Diagnosing vulnerability of variational auto-encoders to adversarial attacks. *arXiv preprint arXiv:2103.06701*, 2021. [2](#), [3](#)
- [22] Anna Kuzina, Max Welling, and Jakub Tomczak. Alleviating adversarial attacks on variational autoencoders with mcmc. *Advances in Neural Information Processing Systems*, 35:8811–8823, 2022. [1](#), [2](#), [3](#)
- [23] Mei Liu, Liangming Chen, Xiaohao Du, Long Jin, and Ming-sheng Shang. Activated gradients for deep neural networks. *IEEE Transactions on Neural Networks and Learning Systems*, 34(4):2156–2168, 2021. [4](#)
- [24] Ziwei Liu, Ping Luo, Xiaogang Wang, and Xiaoou Tang. Deep learning face attributes in the wild. In *Proceedings of International Conference on Computer Vision (ICCV)*, 2015. [5](#)
- [25] Mingfei Lu and Badong Chen. On the adversarial robustness of generative autoencoders in the latent space. *Neural Computing and Applications*, 36(14):8109–8123, 2024. [2](#)
- [26] Jeffrey Pennington, Samuel Schoenholz, and Surya Ganguli. Resurrecting the sigmoid in deep learning through dynamical isometry: theory and practice. *Advances in neural information processing systems*, 30, 2017. [1](#), [2](#)
- [27] Konpat Preechakul, Nattanat Chatthee, Suttisak Wizatwongsa, and Supasorn Suwajanakorn. Diffusion autoencoders: Toward a meaningful and decodable representation. In *Proceedings of the IEEE/CVF conference on computer vision and pattern recognition*, pages 10619–10629, 2022. [1](#), [2](#)
- [28] Alec Radford, Jong Wook Kim, Chris Hallacy, Aditya Ramesh, Gabriel Goh, Sandhini Agarwal, Girish Sastry, Amanda Askell, Pamela Mishkin, Jack Clark, et al. Learning transferable visual models from natural language supervision. In *International conference on machine learning*, pages 8748–8763. PMLR, 2021. [2](#)
- [29] Sirpa Saarinen, Randall Bramley, and George Cybenko. Ill-conditioning in neural network training problems. *SIAM Journal on Scientific Computing*, 14(3):693–714, 1993. [4](#)
- [30] Abhishek Sinha, Mayank Singh, and Balaji Krishnamurthy. Neural networks in an adversarial setting and ill-conditioned weight space. In *Joint European Conference on Machine Learning and Knowledge Discovery in Databases*, pages 177–190. Springer, 2018. [3](#)
- [31] C Szegedy. Intriguing properties of neural networks. *arXiv preprint arXiv:1312.6199*, 2013. [1](#)
- [32] Pedro Tabacof, Julia Tavares, and Eduardo Valle. Adversarial images for variational autoencoders. *arXiv preprint arXiv:1612.00155*, 2016. [1](#)
- [33] Olga Tsymboi, Danil Malaev, Andrei Petrovskii, and Ivan Oseledets. Layerwise universal adversarial attack on nlp models. In *Findings of the Association for Computational Linguistics: ACL 2023*, pages 129–143, 2023. [1](#)
- [34] Arash Vahdat and Jan Kautz. Nvae: A deep hierarchical variational autoencoder. *Advances in neural information processing systems*, 33:19667–19679, 2020. [1](#), [2](#)
- [35] Xin Wang, Yi Qin, Yi Wang, Sheng Xiang, and Haizhou Chen. Reltanh: An activation function with vanishing gradient resistance for sae-based dnns and its application to rotating machinery fault diagnosis. *Neurocomputing*, 363:88–98, 2019. [4](#)
- [36] Matthew Willetts, Alexander Camuto, Tom Rainforth, Stephen Roberts, and Chris Holmes. Improving vaes’ robustness to adversarial attack. *arXiv preprint arXiv:1906.00230*, 2019. [1](#), [2](#), [5](#), [6](#)
- [37] Yaopei Zeng, Yuanpu Cao, Bochuan Cao, Yurui Chang, Jinghui Chen, and Lu Lin. Advi2i: Adversarial image attack on image-to-image diffusion models. *arXiv preprint arXiv:2410.21471*, 2024. [2](#)
- [38] Haomin Zhuang, Yihua Zhang, and Sijia Liu. A pilot study of query-free adversarial attack against stable diffusion. In *Proceedings of the IEEE/CVF Conference on Computer Vision and Pattern Recognition*, pages 2385–2392, 2023. [2](#)

Appendix

A. Proof of Lemma 4.1

We sketch the proof under a simple gradient-based framework. We seek adversarial examples $x_a = x + \epsilon$. Let us denote $\Delta(\cdot) \equiv \|\cdot\|^2$ for simplicity.

Output attack: The classical objective is

$$\operatorname{argmax}_{x_a} \|\mathcal{Y}(x_a) - \mathcal{Y}(x)\|^2.$$

In gradient form, the update for x_a (the perturbation) is:

$$x_a \leftarrow x_a + \eta \nabla_{x_a} \|\mathcal{Y}(x_a) - \mathcal{Y}(x)\|^2.$$

Since $\mathcal{Y}(x_a) = \psi(\phi(x_a))$, by the chain rule:

$$\nabla_{x_a} \|\mathcal{Y}(x_a) - \mathcal{Y}(x)\|^2 = 2(\mathcal{Y}(x_a) - \mathcal{Y})^T \nabla_{x_a} \mathcal{Y}(x_a),$$

where

$$\nabla_{x_a} \mathcal{Y}(x_a) = \mathbf{J}_{\phi(x_a)}^\psi \mathbf{J}_{x_a}^{\phi(x_a)}.$$

If $\sigma_{\min}(\mathbf{J}_{\phi(x_a)}^\psi) \approx 0$, then in certain directions this product is near zero. Hence the gradient vanishes in those directions, limiting the adversarial perturbation.

Lipschitz Maximization Attack (LMA): LMA augments the objective by also maximizing the shift in the latent space, i.e.

$$\operatorname{argmax}_{x_a} \left[\|\mathcal{Y}(x_a) - \mathcal{Y}(x)\|^2 \cdot \|\phi(x_a) - \phi(x)\|^2 \right].$$

Denoting

$$f(x_a) = \|\mathcal{Y}(x_a) - \mathcal{Y}(x)\|^2, \quad g(x_a) = \|\phi(x_a) - \phi(x)\|^2,$$

the new objective is $F(x_a) = f(x_a) g(x_a)$. Its gradient is:

$$\nabla_{x_a} F(x_a) = g(x_a) \nabla_{x_a} f(x_a) + f(x_a) \nabla_{x_a} g(x_a).$$

Here

$$g(x_a) \nabla_{x_a} f(x_a) = \|\phi(x_a) - \phi(x)\|^2 \nabla_{x_a} \|\mathcal{Y}(x_a) - \mathcal{Y}(x)\|^2$$

The first term is the same as the output-attack gradient (up to the scalar factor $g(\epsilon)$). The second term,

$$f(x_a) \nabla_{x_a} g(x_a) = \|\mathcal{Y}(x_a) - \mathcal{Y}(x)\|^2 \nabla_{x_a} \|\phi(x_a) - \phi(x)\|^2,$$

does not involve \mathbf{J}_ϕ^ψ . Thus, even when \mathbf{J}_ϕ^ψ is nearly singular, LMA still has a non-vanishing gradient component via $\nabla_{x_a} g(x_a)$. This pushes x_a to grow in latent space directions, which ultimately can yield a larger change in output

space once the perturbation moves out of the ill-conditioned region.

Hence under $\sigma_{\min}(\mathbf{J}_{\phi(x)}^\psi) \rightarrow 0$, standard output-attack gradients may vanish, but LMA maintains a stronger update signal. Consequently,

$$\Delta(\mathcal{Y}(x), \mathcal{Y}(x_a^{LMA})) \geq \Delta(\mathcal{Y}(x), \mathcal{Y}(x_a^{OA})),$$

as claimed.

B. Proof of Theorem 5.1

Proof. Given ALMA objective in Eq. 14 we have

$$\mathcal{F}(x_a) = \Delta(\mathcal{Y}(x_a), \mathcal{Y}(x)) \sum_{k=1}^{n-1} w_k \Delta(\phi_k(x_a), \phi_k(x))$$

, whose gradient is given by (considering Δ as squared l-2 norm)

$$\begin{aligned} \nabla_{x_a} \mathcal{F}(x_a) &= \sum_{k=1}^{n-1} \nabla_{x_a} (\|\mathcal{Y}(x_a) - \mathcal{Y}(x)\|^2 \cdot \|\phi_k(x_a) - \phi_k(x)\|^2) \\ &= \sum_{k=1}^{n-1} \left(\|\phi_k(x_a) - \phi_k(x)\|^2 \cdot 2(\mathcal{Y}(x_a) - \mathcal{Y}(x))^T \prod_{l=1}^n \mathbf{J}_{\phi_{l-1}}^{\phi_l} \right. \\ &\quad \left. + \|\mathcal{Y}(x_a) - \mathcal{Y}(x)\|^2 \cdot 2(\phi_k(x_a) - \phi_k(x))^T \prod_{l=1}^k \mathbf{J}_{\phi_{l-1}}^{\phi_l} \right) \end{aligned} \quad (15)$$

where we define $\phi_0 := x_a$ to unify the Jacobian product. Given Output space attack objective in Eq. 2 if

$$\begin{aligned} \mathcal{G}(x_a) &= \Delta(\mathcal{Y}(x_a), \mathcal{Y}(x)) = \|\mathcal{Y}(x_a) - \mathcal{Y}(x)\|^2 \\ \nabla_{x_a} \mathcal{G}(x_a) &= 2(\mathcal{Y}(x_a) - \mathcal{Y}(x))^T \prod_{l=1}^n \mathbf{J}_{\phi_{l-1}}^{\phi_l} \end{aligned} \quad (16)$$

Similarly when the latent space attack is considered,

$$\begin{aligned} \mathcal{H}(x_a) &= \Delta(\phi_L(x_a), \phi_L(x)) = \|\phi_L(x_a) - \phi_L(x)\|^2 \\ \nabla_{x_a} \mathcal{H}(x_a) &= 2(\phi_L(x_a) - \phi_L(x))^T \prod_{l=1}^L \mathbf{J}_{\phi_{l-1}}^{\phi_l} \end{aligned} \quad (17)$$

Expressing Eq. 15 in terms of Eq. 16 and Eq. 17 we get

$$\begin{aligned} \nabla_{x_a} \mathcal{F}(x_a) &= \nabla_{x_a} \mathcal{G}(x_a) \sum_{k=1}^{n-1} \|\phi_k(x_a) - \phi_k(x)\|^2 \\ &\quad + \nabla_{x_a} \mathcal{H}(x_a) \|\mathcal{Y}(x_a) - \mathcal{Y}(x)\|^2 \\ &\quad + 2 \cdot \|\mathcal{Y}(x_a) - \mathcal{Y}(x)\|^2 \sum_{k=1, k \neq L}^{n-1} (\phi_k(x_a) - \phi_k(x))^T \cdot \prod_{l=1}^k \mathbf{J}_{\phi_{l-1}}^{\phi_l} \end{aligned} \quad (18)$$

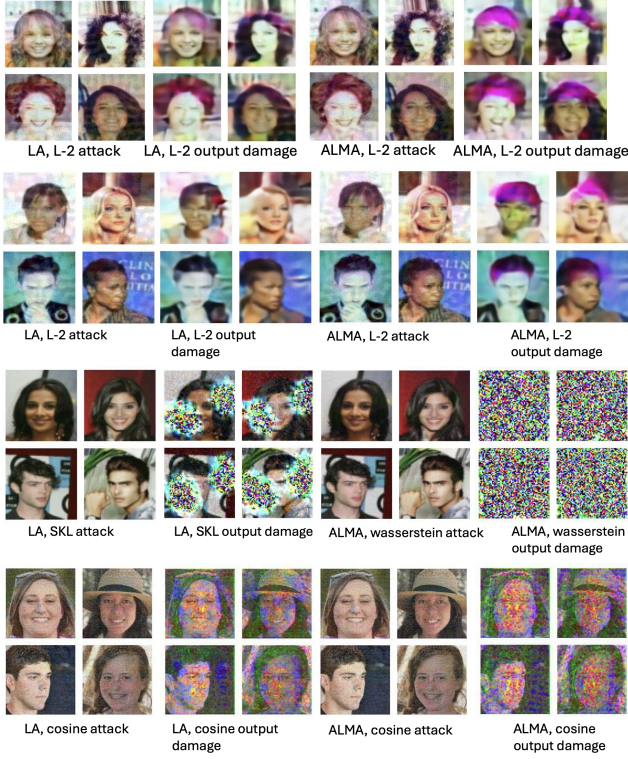


Figure 9. Best performing LA and ALMA universal attacks on β -VAE ($c = 0.07$), TC-VAE ($c = 0.05$), NVAE ($c = 0.05$), and DiffAE ($c = 0.33$), respectively in order from top to bottom.

From the above equation, under ill-conditioning of any intermediate layer in only in the decoder, $\nabla_{x_a} \mathcal{G}(x_a) \rightarrow 0$ and $\nabla_{x_a} \mathcal{F}(x_a) \rightarrow 0$ and hence

$$\|x_a^* - (x_a + \eta \nabla_{x_a} \mathcal{F}(x_a))\| \leq \|x_a^* - (x_a + \eta \nabla_{x_a} \mathcal{G}(x_a))\|$$

Similarly under ill-conditioning of any intermediate layer anywhere in the model including encoder, $\nabla_{x_a} \mathcal{H}(x_a) \rightarrow 0$ and $\nabla_{x_a} \mathcal{F}(x_a) \rightarrow 0$ so that

$$\|x_a^* - (x_a + \eta \nabla_{x_a} \mathcal{F}(x_a))\| \leq \|x_a^* - (x_a + \eta \nabla_{x_a} \mathcal{H}(x_a))\|$$

□

C. Qualitative Plots of LA vs ALMA for Universal Attacks

In Figure 9, we present the qualitative performance of each model, highlighting output damage from both the strongest existing method and our proposed approach. For β -VAE, TC-VAE, and NVAE, our method causes significantly greater damage, which is especially evident in NVAE with its highly ill-conditioned layers (Figure 4(c)). For DiffAE, our method induces slightly more damage than the encoder, primarily due to a significantly ill-conditioned final layer, whereas the remaining layers are well-conditioned.

D. Additional Experimental setup information

While attacking DiffAE, applying Eq. 12 for weight assignment in ALMA (Eq. 14) would result in an extremely low weight $w_{n-1} \approx 0$ for the term $\Delta(\mathcal{Y}(x_a), \mathcal{Y}(x)) \Delta(\phi_{n-1}(x_a), \phi_{n-1}(x))$, effectively suppressing the contribution of the output signal. To mitigate this, we adopt a customized weighting strategy for this case. Rather than using the raw condition number, we heuristically assign a value of 100 to the last layer’s condition number and scale all weights proportionally. This adjustment ensures that ALMA can still exploit the last layer’s ill-conditioning to maximize output damage while maintaining stable gradient propagation.